frontiers in Earth Science

ORIGINAL RESEARCH
published: 17 March 2022
doi: 10.3389/feart.2022.817084

Experiment Study of Porous Fiber Material on Infiltration and Runoff of Winter Wheat Farmland in Huaibei Plain, China

Wei Li[1,2,3], *Shanshan Liu*[3]*, *Tianling Qin*[3]*, *Shangbin Xiao*[1,2], *Chenhao Li*[3,4,5], *Xin Zhang*[3], *Kun Wang*[3] and *Sintayehu A. Abebe*[3]

[1]Engineering Research Center of Eco-Environment in Three Gorges Reservoir Region, Ministry of Education, Yichang, China, [2]College of Hydraulic and Environmental Engineering, China Three Gorges University, Yichang, China, [3]State Key Laboratory of Simulation and Regulation of Water Cycle in River Basin, China Institute of Water Resources and Hydropower Research, Beijing, China, [4]College of Resource Environment and Tourism, Capital Normal University, Beijing, China, [5]Beijing Laboratory of Water Resources Security Beijing Institute of Hydrogeology, Beijing, China

OPEN ACCESS

Edited by:
Sanjeev Kumar Jha,
Indian Institute of Science Education and Research, India

Reviewed by:
Huaiwei Sun,
Huazhong University of Science and Technology, China
Dengfeng Liu,
Xi'an University of Technology, China

***Correspondence:**
Shanshan Liu
liushanshan198705@163.com
Tianling Qin
qintl@iwhr.com

Specialty section:
This article was submitted to Hydrosphere, a section of the journal Frontiers in Earth Science

Received: 17 November 2021
Accepted: 11 January 2022
Published: 17 March 2022

Citation:
Li W, Liu S, Qin T, Xiao S, Li C, Zhang X, Wang K and Abebe SA (2022) Experiment Study of Porous Fiber Material on Infiltration and Runoff of Winter Wheat Farmland in Huaibei Plain, China. Front. Earth Sci. 10:817084. doi: 10.3389/feart.2022.817084

Drought and floods frequently occurred in the Huaibei plain, which was the main factor that restricted agricultural development. We conducted rainfall experiments, which aimed to explore the impacts of porous fiber material (PFM) on the farmland water cycle processes and soil water storage capacity. In this study, we designed two types of rainfall intensities, 4 PFM volumes, 4 growth periods of winter wheat, and a total of 8 experimental groups and 32 rainfall events to evaluate the effects. The result showed that PFM had significantly affected the soil water circulation in the grain-filling period, and the peak flow and runoff decreased maximumly compared with other periods. However, the effect of PFM on surface runoff was slighter in the fallow period, and the peak flow or runoff decreased with the PFM volumes increased (R^2 = –0.92, –0.99). In the 100 and 50 mm/h rainfall intensities, PFM decreased the average values of runoff by (55.2–59.6%) and (57.2–90.2%), reduced peak flow by (62.2–68%) and (64.2–86%), and increased the stable infiltration rate by (13.4–14.3%) and (26.6–41.3%), respectively. After the rainfall experiments ended for 1 h, the surface soil water rapidly infiltrated into PFM, which made the water-storage capacity of PFM groups higher than the control groups by 0.2–11% Vol. Subsequently, PFM increased the water-holding capacity by 0.3–2.3% Vol in the 10–70 cm depth from the heading period to the fallow period. It had a positive relationship between the PFM volumes and the average values of soil water content (R^2 = 0.8, 0.84). In general, PFM could increase infiltration, reduce runoff, and improve the water-storage capacity to alleviate soil water deficit and the risk of farmland drought and floods. It has an excellent application effect in long-duration rainfall.

Keywords: porous fiber material, infiltration, runoff, water-holding capacity, water-storage capacity

INTRODUCTION

Farmland drought and floods frequently occurred globally because the rainfall events were distributed unevenly in time and space. Meanwhile, the change of land use mode and over-development of cultivated land reduces the soil water-holding capacity and aggerates the disaster risk (Karamage et al., 2020; Winkler et al., 2021). Scholars successively studied the effect of porous materials on the water cycle of agricultural farmland (such as straw returning, biochar, and rock wool), aimed to improve the soil structure, increase water-retention capacity, and enhance risk resistance (Saffari et al., 2021; Zhao et al., 2019). Based on the above study, we assumed that the rock wool could redistribute soil water, enhance the water storage capacity, change the soil runoff, and improve the infiltration mechanism of farmland (Cai et al., 2020) (**Figure 1**). Finally, porous fiber material (PFM) reduces the occurrence of farmland drought and flood events and increases risk resistance. Therefore, we conducted extreme rainfall events to explore the impacts of rock wool materials on farmland soil infiltration, runoff, and water-holding capacity.

In the farmland water cycle processes, porosity is considered an important parameter, and it directly influences the soil water distribution and water-holding capacity. At the same time, soil porosity drives the migration of energy and materials and changes the infiltration and runoff mechanism (Helalia, 1993; Huang et al., 2021; Du et al., 2021; Wasko and Nathan, 2019). But the infiltration and runoff of farmland were complex hydrological phenomena; it was the interactive result of rainfall and soil management measures (Yu et al., 2021). Based on the above cognition, porous materials could improve the soil porosity and increase the water-absorbing capacity, water-holding capacity, and water-storage capacity (Sun et al., 2021). Some soil parameters (such as soil porosity and water conductivity) change after the porous materials are embedded in the soil, benefiting the infiltration, and effectively reducing runoff and soil erosion. The internal structural characteristics of porous materials make it easy to absorb and retain water and ultimately achieve a more effective utilization of precipitation (Li et al., 2019; Raimondi and Becciu, 2021).

At present, most scholars have explored the impacts of porous materials on the soil structure (such as the soil porosity, bulk density, water conductivity, etc.) (Humberto, 2017; Dong et al., 2019; Dunkerley, 2021) and revealed its mechanism that the probers materials were how to influence the infiltration process and soil water-holding capacity (Li et al., 2019; Ahmadi et al., 2020; Chen et al., 2020; Yang et al., 2021). Although traditional porous materials increased the infiltration and water-retaining capacity, there were the following defects: blocking soil pores, compacting soil during the application, limiting the improvement range of water-holding capacity (Pu et al., 2019; Zhang F. B. et al., 2019), which would aggravate the soil erosion of farmland in some extreme rainfall events (Werdin et al., 2021; Li et al., 2020). The

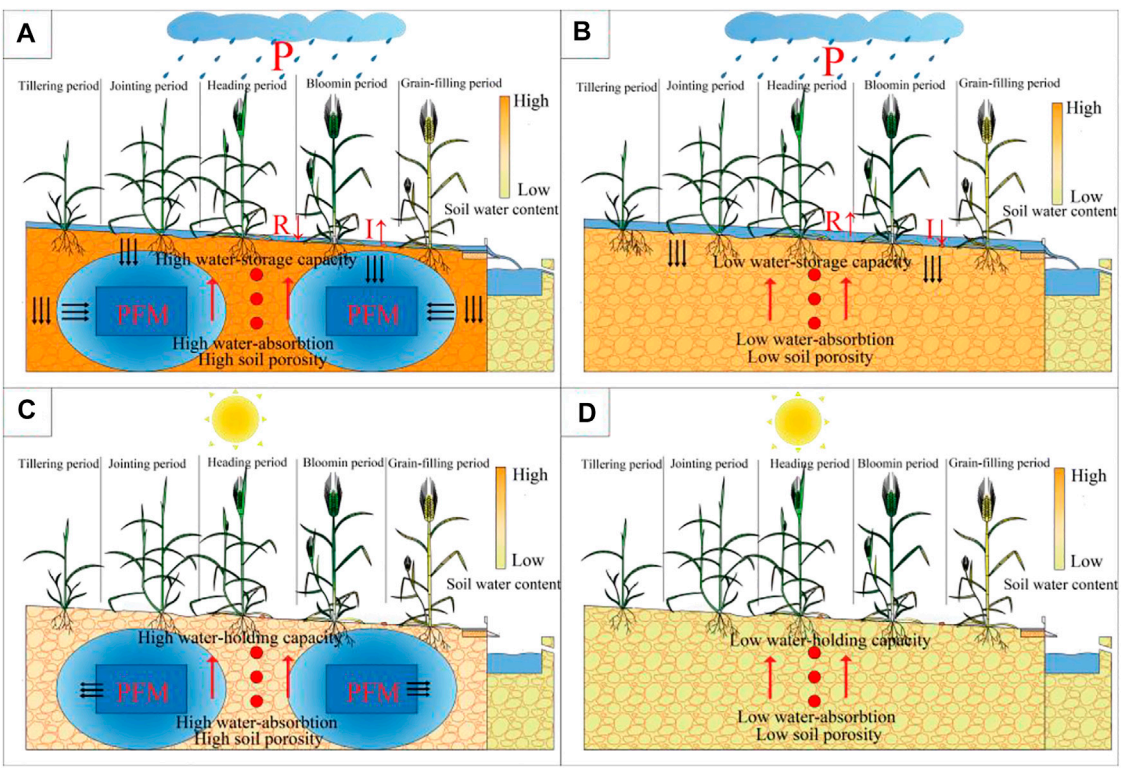

FIGURE 1 | PFM embedding in the farmland increases soil porosity, which benefits the increase of infiltration and the reduction of runoff. **(A–D)** represent the changes of soil water content in the different scenarios, respectively.

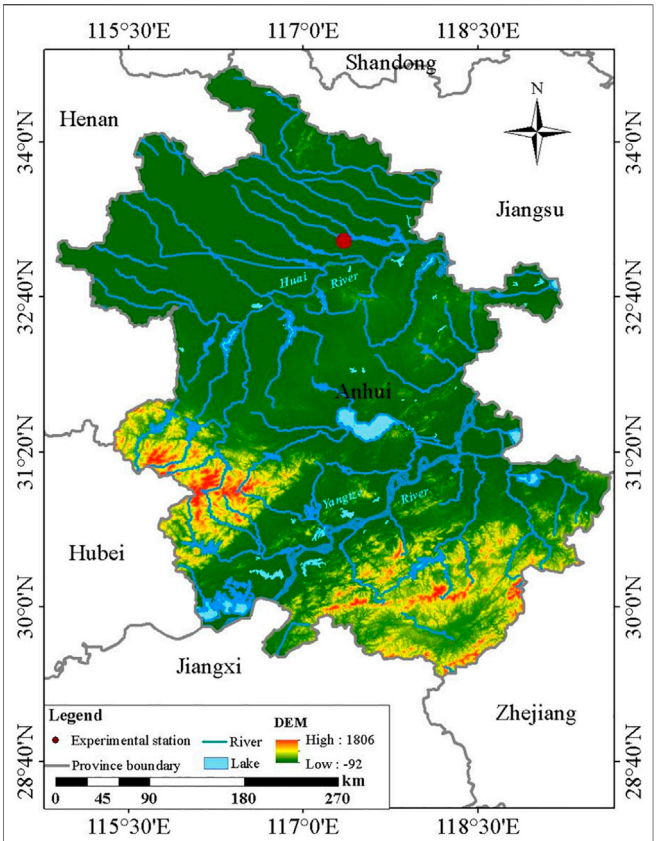

FIGURE 2 | The location of the experiment site and its terrain.

PFM is mainly composed of hydrophilic rock wool, which has stability, high porosity, pressure resistance, and water retention. PFM could quickly absorb water and drain water, which benefits the distribution of water and nutrients on the board uniformly (Bougoul and Boulard, 2006; Titouna and Bougoul, 2013; Choi and Shin, 2019). Because rock wool could regulate the proportion of water, nutrient, and gas in the plant roots' environment, it has been widely used in soilless culture (Savvas and Gruda, 2018). At the same time, the field observation experiments conducted at the woodland and farmland, which confirmed PFM had significant effects on regulating soil water distribution and increasing infiltration (Gu et al., 2020; Lv et al., 2020; Gu et al., 2021; Lv et al., 2021). The above study preliminarily proved that PFM could improve the soil water-holding capacity and had good application in preventing drought and floods disasters (De-Ville et al., 2017). However, most studies were indoor simulation tests of a single factor and a single process, which was difficult to indicate the effect of porous materials on farmland water circulation processes (Pu et al., 2019; Cai et al., 2020; Libutti et al., 2021). In addition, the study about PFM mainly focused on soilless cultivation and green roofs. However, scholars paid little attention to its influence on hydrological characteristics such as farmland soil infiltration and runoff yield processes under extreme rainfall events.

The soil in Huaibei Plain is lime concretion black soil, which has low organic matter content, heavy texture, and poor air permeability. Drought and floods frequently occurred because of the poor soil structure, which was the main factor that restricted agricultural development (Liu. et al., 2017; Bi et al., 2020; Wang et al., 2021). To solve the above problems and extend the utilization of the PFM, we explored the effect of PFM on the infiltration and runoff yield by rainfall experiments. The purposes of this paper are as follows: 1) discovering the impacts of PFM on soil infiltration and runoff; and 2) analyzing the influences of PFM on the water retention capacity of the soil.

STUDY AREA

The experiments were conducted at Wudaogou Hydrological Station (117°21′E, 33°09′N) in Bengbu City, Anhui Province, China. The hydrological station is in the Huai River Basin and Huaibei plain (**Figure 2**). The area experiences a north subtropical and warm temperate semi-humid monsoon climate zone, which is hot and rainy in summer and dry and cold in winter. According to the station data records, the annual average air and surface temperature were 14.7 and 17.9°C, respectively. The annual average precipitation was 890 mm from 1963 to 2017 in this region (Bi et al., 2020; Gou et al., 2020). The maximum rainfall intensity was about 92.4 mm/h, which occurred on June 29, 1997. The main crops include wheat, maize, peanut, soybean, and others. The soil in this region is mainly lime concretion black soil. The effective soil depth is approximately 100 cm, and the soil porosity is about 49.7%.

MATERIAL AND METHODS

Experiment Design

In this study, we set up three factors: two rainfall intensities, four PFM volumes, and four growth periods of winter wheat. Eight experimental groups were designed based on the above factors. The concrete design is shown in **Table 1**.

PFM Volume

The increased goal of soil water-holding capacity was set by 0, 5, 10, and 15%, so the PFM volumes were designed to $V_1 = 0\ m^3$, $V_2 = 1.08\ m^3$, $V_3 = 2.16\ m^3$, and $V_4 = 3.24\ m^3$, respectively. The size of PFM in A2, A3, A4 experimental plots was $0.75 \times 0.45 \times 0.4 \times 8\ m^3$ (length × width × height × block), $1.2 \times 0.45 \times 0.4 \times 10\ m^3$, and $3 \times 0.45 \times 0.4 \times 6\ m^3$, respectively (**Figure 3**), and B2, B3, B4 experimental groups were the same as A2, A3, A4 groups, respectively. PFM volumes can be expressed as (Lv et al., 2020):

$$\delta = \frac{V_1}{V_0} \times \frac{\beta_1 - \beta_0}{\beta_0} \times 100\%$$

$$V_0 = L \times D \times H$$

where δ represents the theoretical increase (%) of soil water-holding capacity; V_1 indicates the PFM volumes in different experimental plots (m^3); V_0 indicates the total volume (m^3) of the effective depth of the experimental plot; β_1 and β_2 are PFM and soil porosity (%), respectively; L, D, and H represent the

TABLE 1 | Scenarios designed and their corresponding experimental plots.

Experimental plots	PFM volume (m^3)	Rainfall intensity (mm/h)	Growth period
A1	V1	100	Heading period
B1	V1	50	
A2	V2	100	Blooming period
B2	V2	50	
A3	V3	100	Grain-filling period
B3	V3	50	
A4	V4	100	Fallow period
B4	V4	50	

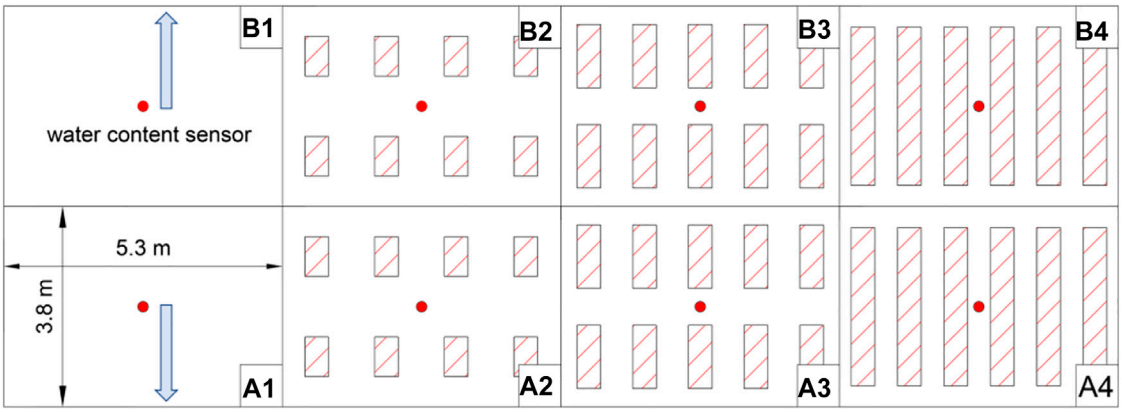

FIGURE 3 | Location of the porous-fiber module in plots and their direction of the slope. A1, A2, A3, and A4 are the experimental plots under 100 mm/h rainfall intensity; B1, B2, B3, and B4 are the experimental plots under 50 mm/h rainfall intensity; the arrow represents the direction of slope, A1~A4 plots have the same direction of the slope; B2-B4 plots are the same as the B1 plot.

length, width, and effective soil depth of the experimental plots, respectively.

Rainfall Intensity

We have referred to the annual rainfall records of the experimental station, and two rainfall intensities were set as P1 = 100 mm/h and P2 = 50 mm/h according to the Grading Standards for Rainfall of China and annual rainfall records, respectively. The rainfall amount of a single experiment was designed to be 150 mm, and the rainfall duration was set as 1.5 and 3 h, respectively.

Growth Periods

We have referred to the water requirement of winter wheat in the Huaibei area, so rainfall experiments were conducted at the heading period (3.24–3.26), the blooming period (4.14–4.17), the grain-filling period (5.8–5.10), and the fallow period (6.8–6.10), respectively. The artificial rainfall was set as the average annual rainfall amount, ensuring that winter wheat grows normally before regreening.

Experimental Plot

The size of experimental plots is 5.3 × 3.8 m^2 with a 3°slope in the north-south direction. The experimental plots and corresponding devices include a rainfall device, wind dodger, water-stop sheep, channel, rain cover, water tank, and water moisture sensor. PFM was embedded in the 30–70 cm depth. Three water sensors were buried in the 20, 40, 60 cm depth in the center of experimental plots, respectively (**Figure 1**).

Date Monitoring

We monitored the variation of soil water content at 8:00 every day. Subsequently, we started rainfall experiments when the soil water content reached 25.0 ± 2.0% Vol at a depth of 20 cm. During rainfall, we recorded the start time of runoff and measured the runoff flow rate at intervals of 5 min. After the rainfall ended, we monitored the variation of soil water content every 1 h for a total of 6 h.

Date Processing

Data were analyzed in SPSS, Excel, and Origin. The significance of the effects of the PFM on the runoff process and water-holding capacity were tested by ANOVA ($p < 0.5$). Finally, we evaluated the impact of PFM on the farmland water cycle by comparing the variation of stable infiltration rate and runoff process.

We could get the cumulative infiltration and infiltration processes according to the runoff processes when we ignored

TABLE 2 | The stable infiltration rate under different growth periods of different experimental plots and evaluation index of fitting performance.

Growth period	Group	A	R2	NSE	RE	Group	A	R2	NSE	RE
Heading period	A1	1.58	0.999	0.999	13.50%	B1	0.61	0.998	0.997	20.90%
	A2	1.58	0.999	0.999	1%	B2	0.82	0.999	0.999	6.30%
	A3	1.54	0.999	0.999	–0.40%	B3	0.77	0.999	0.999	5.40%
	A4	1.56	0.999	0.999	–0.40%	B4	0.83	0.999	0.999	3.30%
Blooming period	A1	1.23	0.999	0.996	16.30%	B1	0.49	0.997	0.993	17.30%
	A2	1.53	0.999	0.999	1.80%	B2	0.79	0.999	0.999	14.90%
	A3	1.5	0.999	0.999	1.80%	B3	0.66	0.999	0.999	3.70%
	A4	1.4	0.999	0.999	0.10%	B4	0.79	0.999	0.999	3.20%
Grain-filling period	A1	1.46	0.999	0.998	22.70%	B1	0.66	0.998	0.997	27.20%
	A2	1.65	0.999	0.999	1.70%	B2	0.83	0.999	0.999	0.80%
	A3	1.66	0.999	0.999	1.40%	B3	0.79	0.999	0.999	-0.20%
	A4	1.66	0.999	0.999	2%	B4	0.83	1	1	0%
Fallow period	A1	1.06	0.999	0.998	0.60%	B1	0.53	0.998	0.996	22%
	A2	1.34	0.999	0.999	5.30%	B2	0.59	0.999	0.998	13.20%
	A3	1.36	0.999	0.999	9.60%	B3	0.68	0.999	0.999	2.70%
	A4	1.49	0.999	0.999	4.90%	B4	0.78	0.999	0.999	8.30%

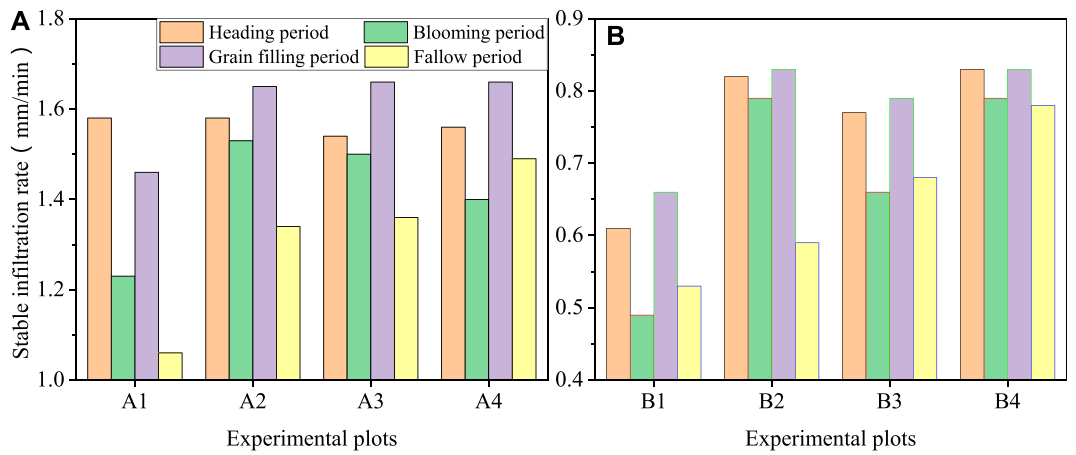

FIGURE 4 | Variations in stable infiltration rate in different rainfall intensity and growth periods. **(A)** and **(B)** in the picture represent the experimental plots under 100 and 50 mm/h rainfall intensity, respectively.

evaporation and the interception by plants. Subsequently, the soil infiltration processes of the experimental plots were fitted by the Philip model and obtained the stable infiltration rate. Finally, we used the R^2, Nash–Sutcliffe efficiency (NSE) coefficient, and relative deviation (RE) between the stable infiltration rate and the minimum infiltration rate to evaluate the performance of the Philip model (Sun et al., 2019; Duan et al., 2021).

$$I(t) = A \times t + S \times t^{0.5}$$

where $I(t)$ represents the theoretical cumulative infiltration amount during the rainfall process, mm; A represents the stable infiltration rate, mm/min; t is the rainfall time, min; S represents a parameter defined as sorptivity, mm/(min$^{0.5}$). Both A and S were determined by the least-square method.

RESULTS

PFM Increase Infiltration

The Philip model was used to fit the infiltration processes when we ignored the plant interception, the R^2 values were more than 0.997 between the stable infiltration rate and the minimum observed infiltration rate, and the Nash–Sutcliffe efficiency (NSE) coefficient values were above 0.993, and the RE values were mostly less than 10% (except the A1 and B1 groups), so the correlation was excellent (**Table 2**). In general, PFM increased the stable infiltration rate by 5.2%, 9.2%, under 100 and 50 mm/h rainfall intensity, respectively, so the PFM increased the stable infiltration rate of experimental plots (**Figure 4**).

PFM increased the stable infiltration rate. The stable infiltration rate of all PFM groups increased by 12.7–61%, compared with the

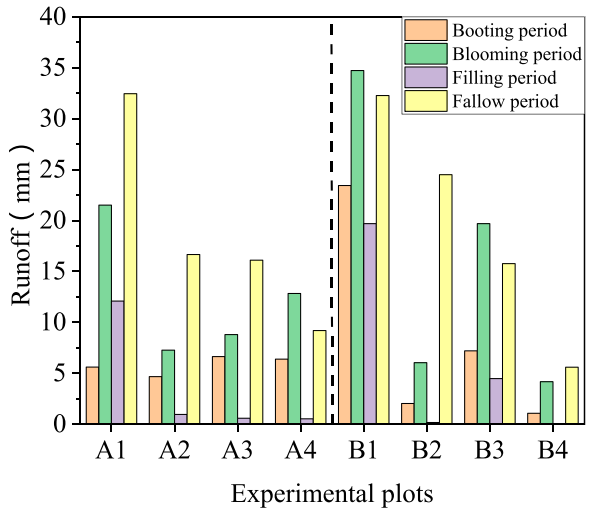

FIGURE 5 | Observed runoff in different plots and growth periods under 100 mm h^{-1} (left) and 50 mm h^{-1} (right) rainfall intensities. A1, A2, A3, and A4 are the experimental plots under 100 mm h^{-1} rainfall intensity; B1, B2, B3, and B4 are the experimental plots under 50 mm h^{-1} rainfall intensity.

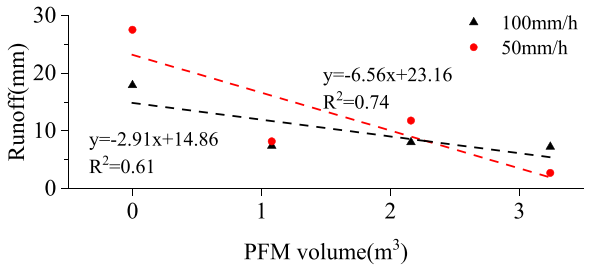

FIGURE 6 | Observed cumulative runoff in different PFM volumes under 100 mm h^{-1} and 50 mm h^{-1} rainfall intensities.

control plots, respectively (except the A1 plot in the heading stage). The minimum infiltration rate by observing increased with the PFM volumes increased too (R^2 = 0.61.0.73). In different growth periods of winter wheat, PFM significantly influenced the variation of stable infiltration rate in the fallow period, and the stable infiltration rate increased with the PFM volumes increased (R^2 = 0.87.0.99), and the stable infiltration rate of the A2, A3, and A4 plots increased by 26.6, 28.7, and 40.6%, respectively, compared with the A1 control plot. In the same way, B2, B3, and B4 groups with the PFM increased by 12.7, 29, and 48.3%, respectively, compared with the B1 control plot. But in the grain-filling period, the range of increase rate only was 13–26.8% when PFM was embedded in the soil.

Analyzing the effect of PFM on infiltration processes from the different rainfall intensities, the increased range of stable infiltration rate after PFM embedding was 13.4–14.3% compared with the A1 control plot under 100 mm/h rainfall intensity, and the stable infiltration rate of PFM experimental groups increased 26.6–41.3% under the 50 mm/h rainfall intensity, compared with the B1 control group. To sum up, we concluded that PFM has excellent applicability under low-intensity or long-duration rainfall.

PFM Decrease Runoff

In general, PFM reduced the runoff volume by 24.1–100% during the rainfall experiment, compared with the control group, respectively (except the A1 plot at the heading period). Total runoff volumes decreased with the PFM volumes increased (R^2 = 0.61.0.74) (**Figures 5**, **6**). Analyzing the impact of PFM on runoff from the growth periods, the runoff volume was the following: the fallow period > the blooming period > the heading period > the grain-filling period. PFM significantly affected runoff during the grain-filling period, and it decreased 77.2–100% at the maximum. In addition, the runoff volumes of PFM groups reduced by 24.1–82.7%, respectively, in the fallow period, compared with the control group, and it comes significantly negatively correlated with the PFM volumes (R^2 = -0.92, -0.99). In the 100 mm/h rainfall intensity, the runoff volume in A2, A3, and A4 groups reduced by 9.9–10.7 mm on average, compared with the A1 control group, respectively, and B2, B3, and B4 groups decreased (15.8–24.8) mm in 50 mm/h (**Figure 5**). PFM has a better application to reduce the runoff in low-intensity and long-duration rainfall.

PFM changes the start time of runoff, but it is not a single variation trend like delaying or moving up. Analyzing the impact of PFM on the start time of runoff from the different growth periods, the start time of runoff was the following: the fallow period < the blooming period < the heading period < the grain-filling period (**Table 3**). In the fallow period, PFM delayed the start time of runoff by 10–55 min compared to the control group (except that the B3 group was earlier than the B1 group by 5 min). In addition, the start time of runoff in the grain-filling period was delayed 27.7–42.1 min compared to other periods, respectively. In the 100 mm/h rainfall intensity, the start time of runoff was 7.5–12.5 min in advance at the PFM experimental plots, compared with the control group. But it had a different change trend under the 50 mm/h rainfall intensity; the runoff volumes of B2 and B4 groups were delayed but the B3 group was advanced, compared with the B1 group.

PFM could improve the water absorption capacity of the soil and reduce peak flow. In total, PFM reduced the peak flow by 24.8–100%, respectively (**Figures 7** and **8**), and it had a positive relationship between the peak flow and the PFM volumes (R^2 = 0.63.0.81). In different growth periods, the peak flow was as follows: the fallow period > the blooming period > the heading period > the grain-filling period. The decrease of peak flow was the largest in the grain-filling period, reaching 88.6–100%, but it was only 29.1–58.8% in the fallow period. In the different rainfall intensity, the peak flow of the A1 group was higher than the B1 group by 24.2%, and B2, B3, and B4 experimental groups increased 29.3, 51.9, and 206.4% by comparing with the A2, A3, and A4 experimental groups, respectively. In **Figure 7**, we could find that the peak flow of runoff positively correlates with the PFM volumes (R^2 = 0.63.0.81), which confirmed PFM had the practical application ability to reduce the risk of farmland flood disaster.

TABLE 3 | Start time of runoff in different experimental stages and plots.

Experimental plots	Time	A1	A2	A3	A4	B1	B2	B3	B4
Jointing period	T	55	10	20	5	20	60	15	125
	ΔT	0	−45	−35	−50	0	40	−5	105
Blooming period	T	25	10	10	15	40	55	15	55
	ΔT	0	−15	−15	−10	0	15	−25	15
Grain-filling period	T	55	55	65	50	75	140	25	—
	ΔT	0	0	10	−5	0	65	-50	—
Fallow period	T	5	15	15	20	20	30	15	75
	ΔT	0	10	10	15	0	10	-5	55
Average	T	35	22.5	27.5	22.5	38.8	71.3	17.5	85
	ΔT	0	−12.5	−7.5	−12.5	0	32.5	−21.3	46.3

T represents the start time of runoff, ΔT represents the variation between the control groups and the PFM experimental groups, — represents no runoff and water fully infiltrated into the soil.

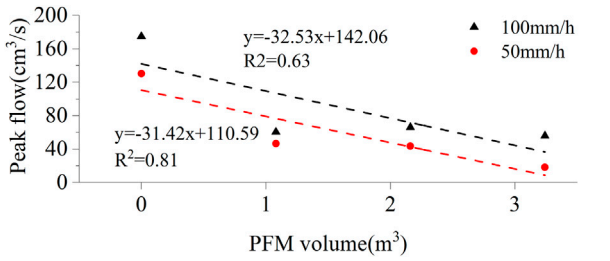

FIGURE 7 | Variation of the peak flow in different PFM volumes under 100 mm h^{-1} and 50 mm h^{-1} rainfall intensities.

PFM Increase the Soil Water-Holding Capacity

PFM could change the distribution of soil water and improve the soil water-holding capacity. In this rainfall experiment, we found that the average soil water content increased by 0.4–2.3% Vol in the 10–70 cm depth, and significantly it had a positive relationship between the soil water content with the PFM volumes (R^2 = 0.8 and 0.84, $p < 0.5$) (**Figure 9**). According to the experimental result, the variation range of soil water content by 25.2–30.9% Vol in the 10–30 cm depth ($p < 0.1$), and the average soil water content of B2 and B4 groups increased but the B3 group reduced by comparing with the B1 groups. Comparing with the 10–30 cm depth, the soil water content had a different variation trend that initially strengthened and subsequently weakened with the PFM volumes increase in the 30–50 cm depth. At the same time, A2, A3, A4, and B2, B3, B4 groups increased by (1.6–2.5% Vol) and (4.5–6.8% Vol) by comparing with the control group, respectively ($p < 0.5$). In the 50–70 cm depth, PFM reduced the soil water content by 0–2.2% Vol (except the B4 group increased by 1% Vol), and the relationship between each other passed the significance test ($p < 0.5$, except the A3 and B3 group).

The impact of PFM on soil water-holding capacity was related to the growth period of the winter wheat (**Figure 10**). The soil water content of the control groups initially decreased and lastly increased as the growth period went and reached a minimum value of 30.8% Vol in the grain-filling period. From the heading period to the fallow period, the increment of soil water content was 0–3.4% Vol in the PFM experimental groups compared with the control groups, respectively. Overall, although in the same condition, the soil water content of B2, B3, and B4 groups were lower than the A2~A4 groups by 0.5–2% Vol (except that the B4 group was higher than the A4 group in the blooming to grain-filling period), the increment of soil water content was higher than the A2, A3, and A4 groups by 0.5–2.6% Vol compared to the respective control groups, respectively.

PFM Increase the Soil Water-Storage Capacity

PFM could increase the soil water storage capacity. After the rainfall experiment ended, PFM increased the soil water content by 0.3–9.8% Vol (except that the A4 group decreased by 2.1% Vol). After rainfall ended for 6 h, the water content of PFM internal increased 0–35.1% Vol (except the B2 plot reduced by 16% Vol, compared to the B1 group), and the rising trend mainly occurred in 0~1 h (**Figure 11**). The soil water content of PFM experimental plots was higher than the control group by 0.2–11% Vol (except that A4 decreased by 1.8% Vol), respectively.

Within 6 h after the rainfall ended, the soil water infiltrated downward rapidly in the depth of 10–30 cm, and the decreased range in the PFM groups was 2.2–10.7% Vol compared with the control group. In the 30–70 cm depth of soil, soil water content decreased slower or even increased by comparing with the surface soil (**Figure 12**). In detail, PFM changed the water distribution in whole plots, and reduced the soil water content by 5.3% Vol and 2.1% Vol on average in the 10–30 cm and 30–50 cm depth of soil, respectively. Although the soil water content in PFM experimental groups had the same variable trend, the decrement was only by 1.1% Vol in the depth of 50–70 cm. So, in a short time after rainfall, the variation range of soil water content decreased with the increase of soil depth. The difference in soil water content shrank between 30 and 70 cm depth when PFM was embedded in the soil. The soil water-storage capacity improved by 0.2–11% Vol in whole plots (except the A3 group was lower than the control group by 1.8% Vol).

DISCUSSION

Porous Fiber Materials Influence the Infiltration and Runoff

The infiltration process of farmland was deeply influenced by some factors such as soil type, rainfall intensity, and initial water

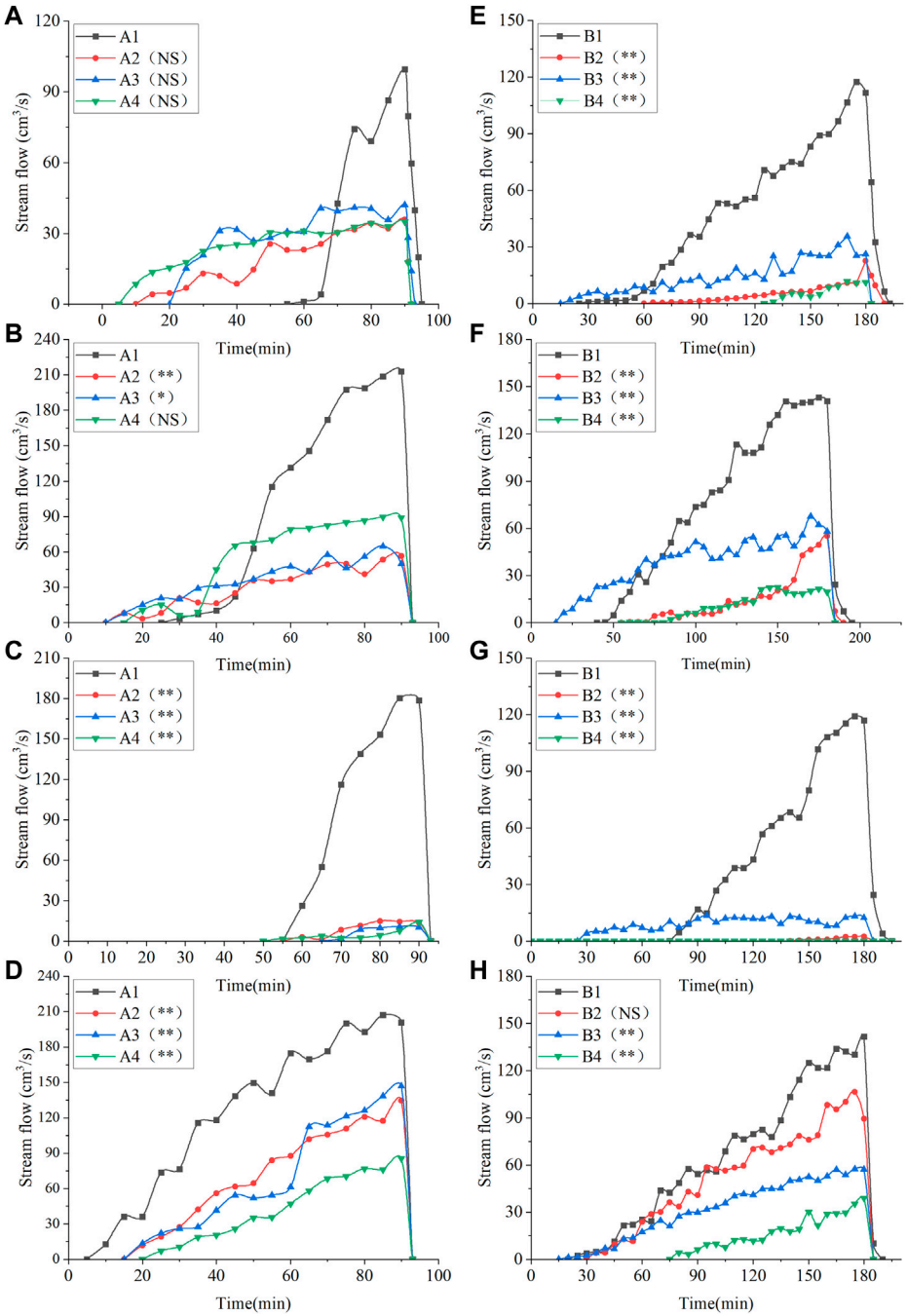

FIGURE 8 | Surface runoff process under different conditions. **(A-D)** The booting period, the blooming period, the grain-filling period, and the fallow period under 100 mm/h rainfall intensity, respectively. **(E-H)** The booting period, blooming period, grain-filling period, and fallow period under 50 mm/h rainfall intensity, respectively; * represents a significant difference in streamflow between the PFM and the control plot at $\alpha = 0.05$; ** represents significant difference between the PFM and the control plots at $\alpha = 0.01$; NS, no significant difference at $\alpha = 0.05$.

content (Humberto, 2017; Dong et al., 2019; Dunkerley, 2021). PFM increased the farmland infiltration rate, which was similar to the research results that some porous materials (such as biochar, straw, and PAM) applied in the farmland (Abrol et al., 2016; Wang et al., 2017). Porous fiber materials changed some soil physical and hydrological characteristics such as soil porosity, water conductivity, aggregate stability, and that the materials including huge pores could provide sufficient space for water storage during rainfall, which benefits the soil infiltration rate increased and reached stable infiltration faster (Gholami et al., 2019; Yu et al., 2021). In the early stage of a rainfall event, the PFM water

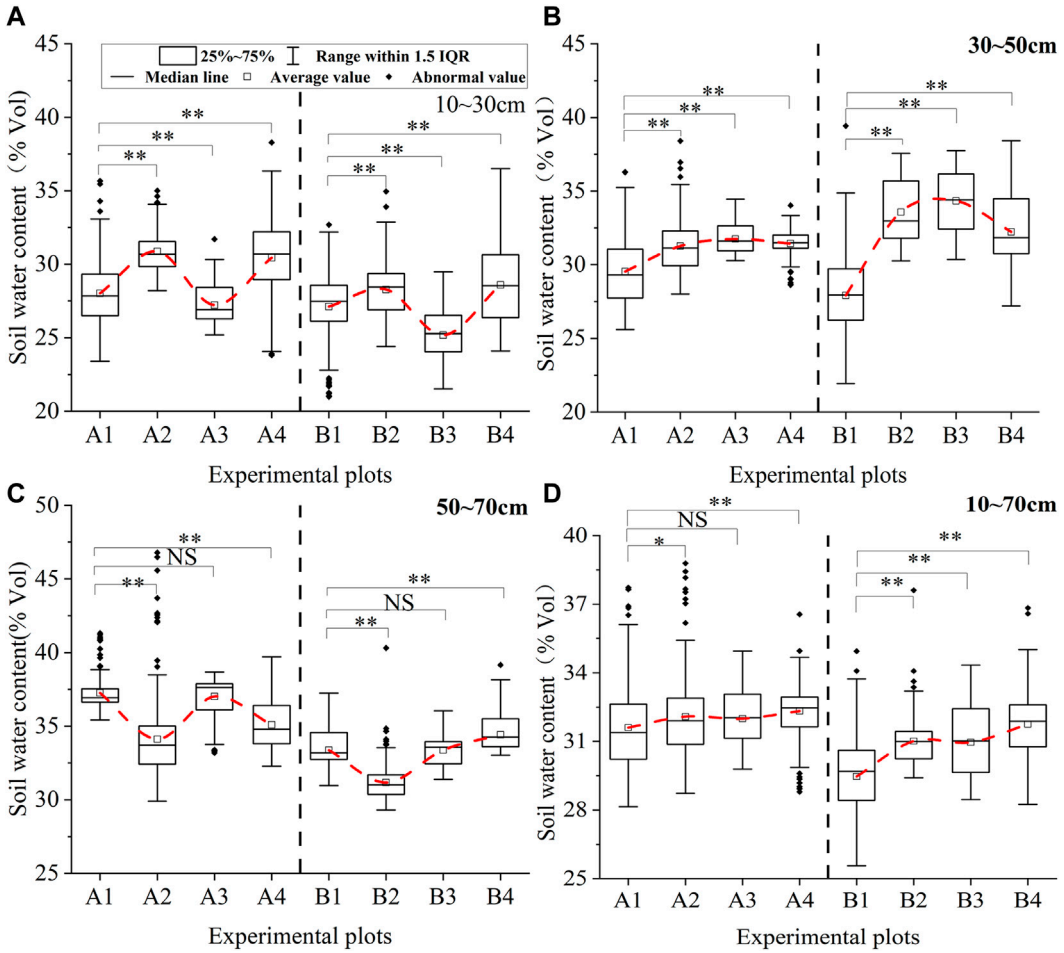

FIGURE 9 | Variations of soil water content in different depths. **(A-D)** The different depths of the soil, * represents a significant difference in streamflow between the PFM and the control plots at α = 0.05; ** represents a significant difference between the PFM and the control plots at α = 0.01; NS represents no significant difference at α = 0.05.

content was often lower than the soil water content in the same depth, which would make soil water suction in the PFM groups higher than the control groups during rain. PFM would actively absorb the free water when the soil pore saturated during the long-duration rain because the difference in potential energy, and the water absorption capacity of hydrophilic rock wool increases with the irrigation time increase, so it can enhance the effect on the infiltration process in a long duration rainfall (Lv et al., 2021). Subsequently, the infiltration rate would reach a stable value faster, which is the reason why the RE values of the control group are higher than the PFM groups.

Some researchers confirmed that green roofs filled with porous materials could reduce the runoff and the peak flow because the free water in the soil permeated into the porous materials and stored in the drainage layer during rainfall (Stovin., 2010). Similarly, porous materials should have the same advantages in the farmland, and Patrick and Vikas thought it could improve some soil structure parameters (such as porosity, texture, and particle size distribution), which benefited by reducing the surface runoff (Abrol et al., 2016; Nyambo et al., 2018; Li et al., 2019). However, biochar was easy to be washed off by runoff or block the soil pores in some extreme rainfall events, which led to the intensification of farmland floods (Peng et al., 2016). But PFM does not have the above shortcomings in practical application due to the difference in its layout mode (Yu et al., 2021). In nature, the formation and growth of surface runoff depend more on the relationship between rainfall intensity and soil infiltration rate (Zhao X. et al., 2014; Werdin et al., 2021). We have explained why the PFM could affect the infiltration process, so PFM inevitably reduced runoff when the rainfall intensity was stable.

PFM affected the starting time and processes of runoff. The effects of different PFM volumes on the start time of runoff were not a single variation trend during the rain, which was different from Zhou et al. in the biochar application (Zhou et al., 2020).

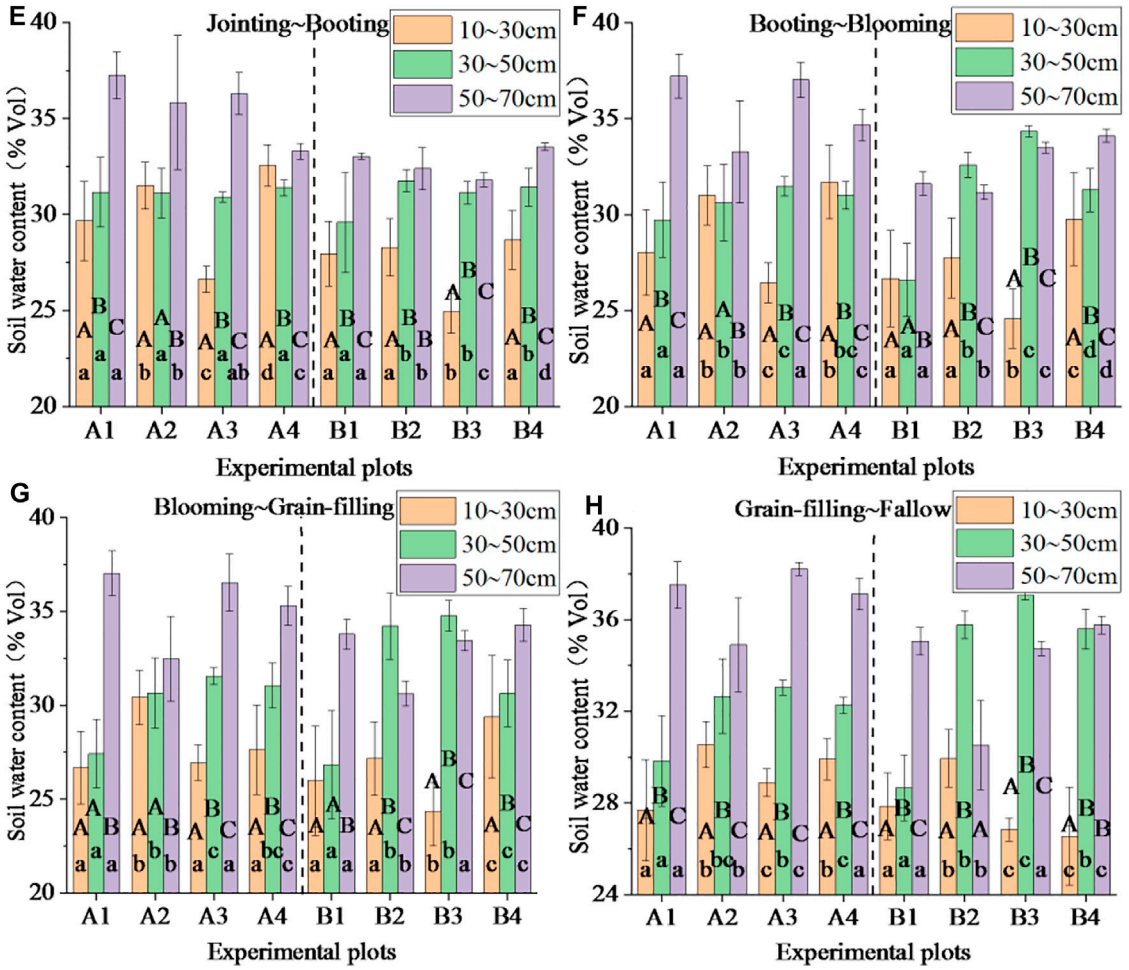

FIGURE 10 | Variations in soil water content in different growth periods and depths. **(E-H)** represent the different periods; a, b, c, d indicate the significant difference between the different depths at 0.05; **(A-C)** indicate the significant difference between different PFM volumes. PFM increases the soil water-storage capacity.

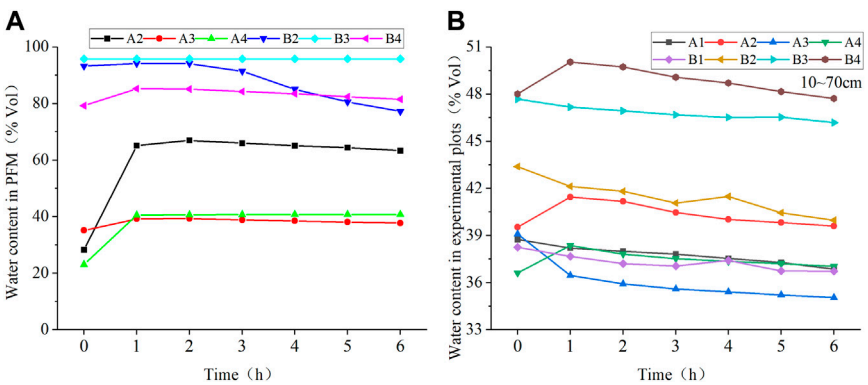

FIGURE 11 | Redistributions of soil and PFM water content in experimental plots from 1 to 6 h after rainfall (The letters **(A)** and **(B)** in the top left corner represent PFM and experimental plots, respectively.

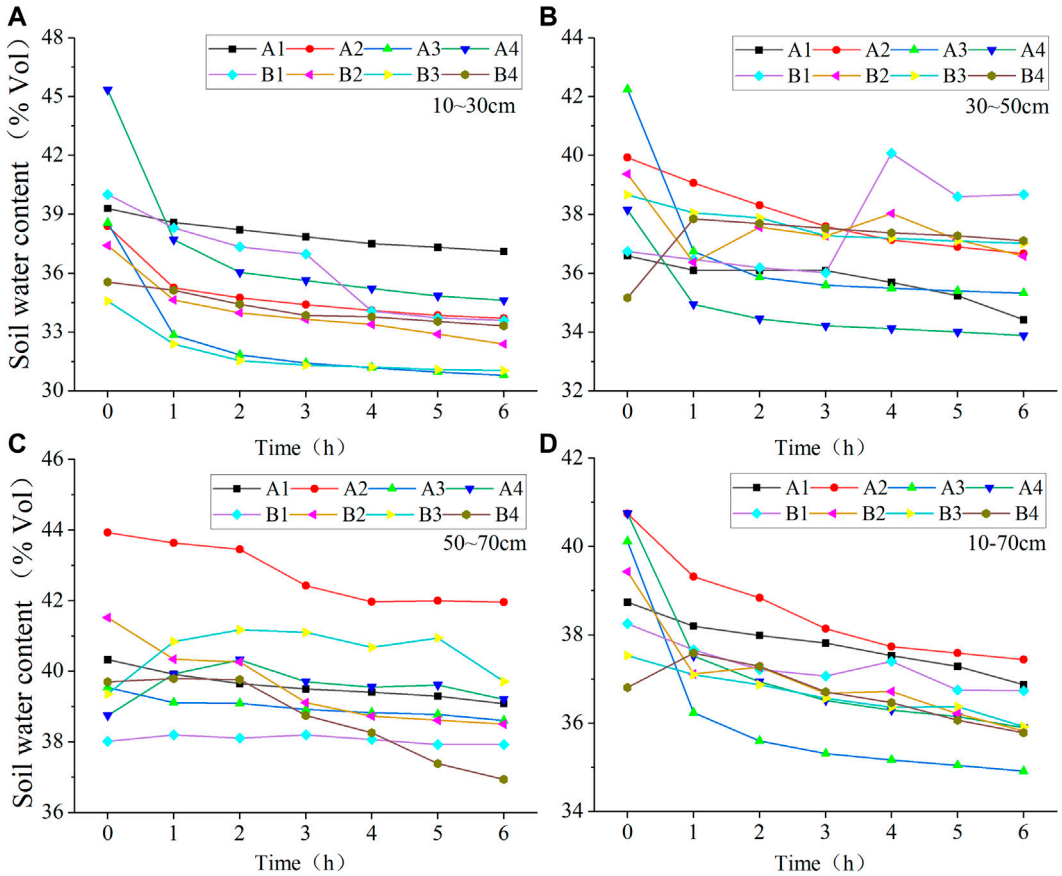

FIGURE 12 | Redistributions of soil water content in experimental plots at 10–70 cm depth from 1 to 6 h after rainfall ended (The letters **(A-D)** in the top left corner represent the different depths of soil).

The start time of runoff increased with the increase of biochar amount, this is mainly because biochar in the surface soil could absorb water and quickly respond to the infiltration processes, and delay the formation of runoff. However, PFM was difficult to respond to the formation of surface runoff in time due to the 30–70 cm depth of layout. Similarly, biochar could increase the water-holding capacity, which meant that the initial water content of the PFM groups before rainfall was higher than the control group. The porous materials have huge pores that can store water in rainfall and release water in drought, which made the soil water retain a high level, and directly affect the start time of runoff or even in advance like the B3 group (Razzaghi et al., 2020). Subsequently, surface soil water content would reach the threshold required for runoff faster, and the wetting front moved further down, finally, the surface runoff was accelerated to be formed (Song and Wang, 2019; Zhang J. L. et al., 2019; Rascon-Ramos et al., 2021), but it might be inappropriate in short-duration rain (Choi and Shin, 2019). PFM would actively absorb the free water to alleviate the flood disaster risk in long-duration rainfall after the soil water is closed to saturation, or the soil suction is less than 75 cm (Lv et al., 2021), so it has the different varied trend after the rainfall ended for 1 h under the 100 mm/h and 50 mm/h rainfall intensity. Therefore, the applicability of PFM embedding is better under continuous or long-duration rainfall (**Figure 8**).

The effect of PFM on runoff has a significant variation in the grain-filling period because the raindrops damaged the surface aggregate structure and promoted soil erosion (Ao et al., 2019; Ahmadi et al., 2020). In addition, the collapse plants absorbed a large amount of raindrops' energy and slowed down the above process. Meanwhile, winter wheat consumed large amounts of water for grouting, which made the initial soil water content lower than other periods and delayed the start time of runoff on a large scale (Zhang J. L. et al., 2019). The raindrop kinetic energy directly made soil particles separate in the fallow period, and the part of soil particle washed and taken away by runoff, another was precipitated on the soil surface to form a sealing plane, and reduced the infiltration rate and accelerated the formation and growth of runoff (Sadeghi et al., 2016; Yao et al., 2018).

The farmland runoff is usually uncertain in time and space in the natural rainfall because of the interaction of some factors such as the initial water content, rainfall intensity, and surface roughness. PFM embedding might cause a slight negative impact during short-duration rainfall. The application on farmland drainage is better in continuous rainfall events.

Porous Materials Influence the Soil Water-Holding Capacity and the Water-Storage Capacity

PFM increases the soil water-holding capacity and changes soil water distribution, the same as the results of other studies. For example, rock wool embedding in the forest land could increase the soil water content by 29.29% after a long-duration drought (Gu et al., 2020). The key to the above phenomenon was porous materials could fully absorb water during rainfall and increase soil water-storage capacity (Mollinedo et al., 2015). After the rainfall ended, soil water infiltrated, evaporated, or absorbed by the roots and gradually decreased to the unsaturated. At that time, the soil suction was much higher than PFM, which made PFM continuously release water to alleviate soil water deficit (Gu et al., 2020; Lv et al., 2021).

After the rainfall experiments, the water rapidly exchanged between the PFM and the surrounding soil on a large scale because of the various potential energy (Lv et al., 2021). The surface soil water decreased quickly, but the deep soil changed slowly. The water absorption capacity of hydrophilic rock wool increased with irrigation time (Choi and Shin, 2019). The surface and deep soil water infiltrated the PFM from vertical and horizontal directions. PFM water content increased rapidly by 0–35.1% Vol under 100 mm/h rainfall intensity after the rainfall ended for 1 h and remained stable at high levels because of the different matrix suction and the geopotential conditions (Lv et al., 2020). PFM had sufficient infiltration time under the long-duration rainfall, so it significantly has the better appliance effects under the 50 mm/h, which benefits the improvement of the soil water storage (Choi and Shin, 2019; Kołodziej et al., 2020). In general, the variation of soil moisture is an exponential downward trend during the long-dated observation. The mutations of soil water occasionally might occur after rainfall in some time because the soil exists in the heterogeneous mixture in the local area, which makes the soil hydraulic characteristics different; therefore, the B1 group rises significantly after rainfall.

PFM has evenly arranged fiber composition (one-way or cross), improving infiltration processes, and water-holding capacity. Rock wool material could naturally and continuously penetrate, buffer, and discharge rainwater and effectively achieve rainwater absorption and utilization (Wanko et al., 2016). However, the roots of winter wheat are generally short and mainly distributed in the surface soil (Nosalewicz and Lipiec, 2014; Figueroa-Bustos et al., 2018), and it is difficult to root into the PFM, so we analyzed the effect of PFM on soil water-holding capacity from the variation of soil water content. In detail, PFM steadily water to supply soil after rain and led to decreased hydraulic conductivity and increased soil water suction, further alleviating soil water deficit (Bougoul et al., 2005). In this process, the diffusion ability in vertical and horizontal directions gradually decreased from the center of the PFM embedding position to the surrounding, and shrank the gap of the soil water content in the vertical and improved the water-holding capacity (Gu et al., 2020). PFM acted as an intermediate medium to redistribute water of the surrounding in the 30–70 cm depth, which would also affect the water exchange at other depths, and adjusted the water potential difference to improve the water-holding capacity, this was similar to that PFM plays a role in regulating the root of the environment in the soilless culture (AcuA et al., 2013; Graceson et al., 2013; Narzari et al., 2017).

In summary, PFM can effectively increase soil infiltration, reduce runoff, and improve soil water storage capacity. Although porous fiber materials are currently used in soilless culture, they can adjust the proportion of water, fertilizer, and air in crop roots, which benefits plant growth well (Savvas and Gruda, 2018). In general, the expense of PFM restricted its application on a large scale at present, and the average price of a PFM ranges from ¥1,000 to ¥2,000 m^{-3}, so we can use it in intensive agriculture or economic crop planting. At the same time, we must realize that PFM cannot create water or reduce the soil water consumption of farmland. It only plays a role in enhancing soil water storage capacity to delay drought events. To effectively achieve the drought disaster risk reduction in the extremely dry years, improving the soil water content may be necessary through PFM embedding and irrigation system interaction.

CONCLUSION

PFM influences soil infiltration and water exchanging by establishing a hydraulic connection with the surrounding soil. Based on the above assumptions, we experimented with the growth period of winter wheat to explore the effects of PFM embedding on the farmland water cycle processes. The result showed that PFM could absorb a large amount of free water in saturated soil during rain. Subsequently, it increased the soil infiltration rate and reduced the runoff. After rainfall, PFM could regulate the water redistribution and improve water-holding capacity to alleviate soil water deficit. The above effects increased with the PFM volumes increased. In general, the expense of PFM restricted its application on a large scale at present, and the average price of a PFM ranges from ¥1,000 to ¥2,000 m^{-3}, so we can expand the application to intensive agriculture and economic crops in the farmland. Furthermore, we believe that PFM will have excellent application effects in soil and water conservation, sponge city, green roof, potting, etc.

DATA AVAILABILITY STATEMENT

The original contributions presented in the study are included in the article/Supplementary Material. Further inquiries can be directed to the corresponding authors.

AUTHOR CONTRIBUTIONS

WL, SL, and TQ conceived the main idea of this manuscript. SX, CL, XZ, and KW designed and performed the experiment. SA

helped to revise the manuscript. WL wrote the manuscript and all authors contributed to improving the manuscript.

FUNDING

This research was supported by the National Key Research and Development Project (Grant No. 2017YFA0605004), the National Science Fund Project for Distinguished Young Scholars (Grant No. 51725905), and the National Science Fund Project (Grant No. 52130907).

ACKNOWLEDGMENTS

We thank the reviewers for their useful comments and suggestions.

REFERENCES

Abrol, V., Ben-Hur, M., Verheijen, F. G. A., Keizer, J. J., Martins, M. A. S., Tenaw, H., et al. (2016). Biochar Effects on Soil Water Infiltration and Erosion under Seal Formation Conditions: Rainfall Simulation experiment. *J. Soils Sediments* 16, 2709–2719. doi:10.1007/s11368-016-1448-8

Acuña, R. A., Bonachela, S., Magán, J. J., Marfà, O., Hernández, J. H., and Cáceres, R. (2013). Reuse of Rockwool Slabs and Perlite Grow-Bags in a Low-Cost Greenhouse: Substrates' Physical Properties and Crop Production. *Scientia Horticulturae* 160, 139–147. doi:10.1016/j.scienta.2013.05.031

Ahmadi, S. H., Ghasemi, H., and Sepaskhah, A. R. (2020). Rice Husk Biochar Influences Runoff Features, Soil Loss, and Hydrological Behavior of a Loamy Soil in a Series of Successive Simulated Rainfall Events. *Catena* 192, 104587. doi:10.1016/j.catena.2020.104587

Ao, C., Yang, P., Zeng, W., Chen, W., Xu, Y., Xu, H., et al. (2019). Impact of Raindrop Diameter and Polyacrylamide Application on Runoff, Soil and Nitrogen Loss via Raindrop Splashing. *Geoderma* 353, 372–381. doi:10.1016/j.geoderma.2019.07.026

Bi, W., Weng, B., Yan, D., Wang, M., Wang, H., Wang, J., et al. (2020). Effects of Drought-Flood Abrupt Alternation on Phosphorus in Summer maize farmland Systems. *Geoderma* 363, 114147. doi:10.1016/j.geoderma.2019.114147

Bougoul, S., and Boulard, T. (2006). Water Dynamics in Two Rockwool Slab Growing Substrates of Contrasting Densities. *Scientia Horticulturae* 107, 399–404. doi:10.1016/j.scienta.2005.11.007

Bougoul, S., Ruy, S., de Groot, F., and Boulard, T. (2005). Hydraulic and Physical Propertiesof Stonewool Substrates in Horticulture. *Scientia Horticulturae* 104, 391–405. doi:10.1016/j.scienta.2005.01.018

Cai, W., Huang, H., Chen, P. N., Huang, X. L., and GauravPan, S. Z. (2020). Effects of Biochar from Invasive weed on Soil Erosion under Varying Compaction and Slope Conditions: Comprehensive Study Using Flume Experiments. *Biomass Convers. Biorefinery*. doi:10.1007/s13399-020-00943-3

Chen, X. A., Liang, Z. W., Zhang, Z. Y., and Zhang, L. (2020). Effects of Soil and Water Conservation Measures on Runoff and Sediment Yield in Red Soil Slope Farmland under Natural Rainfall. *Sustainability* 12, 3417. doi:10.3390/su12083417

Choi, Y. B., and Shin, J. H. (2019). Analysis of the Changes in Medium Moisture Content According to a Crop Irrigation Strategy and the Medium Properties for Precise Moisture Content Control in Rock Wool. *Hortic. Environ. Biotechnol.* 60, 337–343. doi:10.1007/s13580-019-00134-8

De-Ville, S., Menon, M., Jia, X. D., Reed, G., and Stovin, V. (2017). The Impact of green Roof Ageing on Substrate Characteristics and Hydrological Performance. *J. Hydrol.* 547, 332–344. doi:10.1016/j.jhydrol.2017.02.006

Dong, Q. G., Han, J. C., Zhang, Y., Li, N., Lei, N., Sun, Z. H., et al. (2019). Water Infiltration of Covering Soils with Different Textures and Bulk Densities in Gravelmulched Areas. *Appl. Ecol. Environ. Res.* 17, 14039–14052. doi:10.15666/aeer/1706_1403914052

Du, M. C., Zhang, J. Y., Elmahdi, A., Wang, Z. L., Yang, Q. L., Liu, H. W., et al. (2021). Variation Characteristics and Influencing Factors of Soil Moisture Content in the Lime Concretion Black Soil Region in Northern Anhui. *Water* 13, 2251. doi:10.3390/w13162251

Duan, M. L., Liu, G. H., Zhou, B. B., Chen, X. P., Wang, Q. J., Zhu, H. Y., et al. (2021). Effects of Modified Biochar on Water and Salt Distribution and Water-Stable Macro-Aggregates in Saline-Alkaline Soil. *J. Soils Sedim.* 21, 2192–2202. doi:10.1007/s11368-021-02913-2

Dunkerley, D. (2021). The Importance of Incorporating Rain Intensity Profiles in Rainfall Simulation Studies of Infiltration, Runoff Production, Soil Erosion, and Related Landsurface Processes. *J. Hydrol.* 603, 126834. doi:10.1016/j.jhydrol.2021.126834

Figueroa-Bustos, V., Palta, J. A., Chen, Y. L., and Siddique, K. H. M. (2018). Characterization of Root and Shoot Traits in Wheat Cultivars with Putative Differences in Root System Size. *Agronomy-Basel* 8, 109. doi:10.3390/agronomy8070109

Gholami, L., Karimi, N., and Kavian, A. (2019). Soil and Water Conservation Using Biochar and Various Soil Moisture in Laboratory Conditions. *Catena* 182, 104151. doi:10.1016/j.catena.2019.104151

Gou, Q. Q., Zhu, Y. H., Horton, R., Lu, H. S., Wang, Z. L., Su, J. B., et al. (2020). Effect of Climate Change on the Contribution of Groundwater to the Root Zone of winter Wheat in the Huaibei Plain of China. *Agric. Water Manage.* 240. doi:10.1016/j.agwat.2020.106292

Graceson, A., Hare, M., Monaghan, J., and Hall, N. (2013). The Water Retention Capabilities of Growing media for green Roofs. *Ecol. Eng.* 61, 328–334. doi:10.1016/j.ecoleng.2013.09.030

Gu, J. Y., Fang, W., Gao, J., Yan, S. X., Feng, G. L., Liu, C. X., et al. (2020). Improving Soil Water Retention Capacity of Economic forest Using Rock Wool in Hilly Area. *Agric. Res. Arid Areas* 38 (3), 10–18. doi:10.7606/j.issn.1000-7601.220.03.02

Gu, J. Y., Shao, S., Deng, Y. J., Yu, C. B., Chen, J. H., Qin, H., et al. (2021). Response of Growth and Physiological Indicators of Lycopersicone Sculentum to Water Stress Relieved by Rock Wool. *J. Zhejiang A&F Univ.* 38 (2), 311–319. doi:10.11833/j.issn.2095-0756.20200221

Helalia, A. M. (1993). The Relation between Soil Infiltration and Effective Porosity in Different Soils. *Agric. Water Manag.* 24, 39–47. doi:10.1016/0378-3774(93)90060-N

Huang, W., Du, J. X., Sun, H., Zhou, C. Y., Liu, Z., and Zhang, L. H. (2021). New Polymer Composites Improve Silty Clay Soil Microstructure: An Evaluation Using NMR. *Land Degradat. Devel.* 32, 3272–3281. doi:10.1002/ldr.3983

Humberto, B. C. (2017). Biochar and Soil Physical Properties. *Soil Sci. Soc. America J.* 81, 687–711. doi:10.2136/sssaj2017.01.0017

Kołodziej, B., Bryk, M., and Otremba, K. (2020). Effect of Rockwool and lignite Dust on Physical State of Rehabilitated post-mining Soil. *Soil Tillage Res.* 199, 104603. doi:10.1016/j.still.2020.104603

Li, Y. Y., Feng, G., Tewolde, H., Yang, M. Y., and Zhang, F. B. (2020). Soil, Biochar, and Nitrogen Loss to Runoff from Loess Soil Amended with Biochar under Simulated Rainfall. *J. Hydrol.* 591, 125318. doi:10.1016/j.jhydrol.2020.125318

Li, Y. Y., Zhang, F. B., Yang, M. Y., and Zhang, J. Q. (2019). Effects of Adding Biochar of Different Particle Sizes on Hydro-Erosional Processes in Small Scale Laboratory Rainfall Experiments on Cultivated Loessial Soil. *Catena* 173, 226–233. doi:10.1016/j.catena.2018.10.021

Libutti, A., Francavilla, M., and Monteleone, M. (2021). Hydrological Properties of a Clay Loam Soil as Affected by Biochar Application in a Pot Experiment. *Agronomy* 11, 489. doi:10.3390/agronomy11030489

Liu, S. M., Wang, H., Yan, D. H., Qin, T. L., Wang, Z. L., and Wang, F. X. (2017). Crop Growth Characteristics and Waterlogging Risk Analysis of Huaibei Plain in Anhui Province, China. *J. Irrigation Drainage Eng.* 143, 04017042. doi:10.1061/(ASCE)IR.1943-4774.0001219

Lv, Z. Y., Qin, T. L., Liu, S. S., Nie, H. J., Liu, F., and Wang, J. W. (2020). Porous-fiber Module Increases Infiltration and Reduces Runoff. *Agron. J.* 112, 4420–4436. doi:10.1002/agj2.20317

Lv, Z. Y., Qin, T. L., Wang, Y., Liu, S. S., Nie, H. J., and Wang, J. W. (2021). Hydraulic Properties of the Porous-Fiber Module and its Effects on Infiltration and Runoff. *Agron. J.* 113, 2913–2925. doi:10.1002/agj2.20630

Mollinedo, J., Schumacher, T. E., and Chintala, R. (2015). Influence of Feedstocks and Pyrolysis on Biochar's Capacity to Modify Soil Water Retention Characteristics. *J. Anal. Appl. Pyrolysis* 114, 100–108. doi:10.1016/j.jaap.2015.05.006

Narzari, R., Bordoloi, N., Sarma, B., Gogoi, L., Gogoi, N., Borkotoki, B., et al. (2017). Fabrication of Biochars Obtained from Valorization of Biowaste and Evaluation of its Physicochemical Properties. *Bioresour. Technol.* 242, 324–328. doi:10.1016/j.biortech.2017.04.050

Nosalewicz, A., and Lipiec, J. (2014). The Effect of Compacted Soil Layers on Vertical Root Distribution and Water Uptake by Wheat. *Plant and Soil* 375, 229–240. doi:10.1007/s11104-013-1961-0

Nyambo, P., Taeni, T., Chiduza, C., and Araya, T. (2018). Effects of Maize Residue Biochar Amendments on Soil Properties and Soil Loss on Acidic Hutton Soil. *Agronomy* 8, 256. doi:10.3390/agronomy8110256

Peng, X., Zhu, Q. H., Xie, Z. B., Darboux, F., and Holden, N. M. (2016). The Impact of Manure, Straw and Biochar Amendments on Aggregation and Erosion in a Hillslope Ultisol. *Catena* 138, 30–37. doi:10.1016/j.catena.2015.11.008

Pu, S. H., Li, G. Y., Tang, G. M., Zhang, Y. S., Xu, W. L., Li, P., et al. (2019). Effects of Biochar on Water Movement Characteristics in sandy Soil under Drip Irrigation. *J. Arid Land* 11, 740–753. doi:10.1007/s40333-019-0106-6

Raimondi, A., and Becciu, G. (2021). Performance of Green Roofs for Rainwater Control. *Water Res. Manag.* 35, 99–111. doi:10.1007/s11269-020-02712-3

Rascon-Ramos, A. E., Martinez-Salvador, M., Sosa-Perez, Gl., Villarreal-Guerrero, F., Pinedo-Alvarez, A., and Santellano-Estrada, E. (2021). Hydrological Behavior of a Semi-dry forest in Northern Mexico: Factors Controlling Surface Runoff. *Arid Land Res. Manage.* 35, 83–103. doi:10.1080/15324982.2020.1783026

Razzaghi, F., Obour, P. B., and Arthur, E. (2020). Does Biochar Improve Soil Water Retention? A Systematic Review and Meta-Analysis. *Geoderma* 361. doi:10.1016/j.geoderma.2019.114055

Sadeghi, S. H. R., Sharifi, M. E., and Khaledi, D. A. (2016). Effects of Subsequent Rainfall Events on Runoff and Soil Erosion Components from Small Plots Treated by Vinasse. *Catena* 138, 1–12. doi:10.1016/j.catena.2015.11.007

Saffari, N., Hajabbasi, M. A., Shirani, H., Mosaddeghi, M. R., and Owens, G. (2021). Influence of Corn Residue Biochar on Water Retention and Penetration Resistance in a Calcareous Sandy Loam Soil. *Geoderma* 383. doi:10.1016/j.geoderma.2020.114734

Savvas, D., and Gruda, N. (2018). Application of Soilless Culture Technologies in the Modern Greenhouse Industry – A Review. *Eur. J. Hortic. Sci.* 83, 280–293. doi:10.17660/eJHS.2018/83.5.2

Song, S., and Wang, W. (2019). Impacts of Antecedent Soil Moisture on the Rainfall-Runoff Transformation Process Based on High-Resolution Observations in Soil Tank Experiments. *Water* 11, 296. doi:10.3390/w11020296

Stovin, V. (2010). The Potential of green Roofs to Manage Urban Stormwater. *Water Environ. J.* 24, 192–199. doi:10.1111/j.1747-6593.2009.00174.x

Sun, C. X., Wang, D., Shen, X. B., Li, C. H., Liu, J., Lan, T., et al. (2021). Effects of Biochar, Compost and Straw Input on Root Exudation of Maize (Zea mays L.): From Function to Morphology. *Agricult. Ecosyst. Environ.* 308. doi:10.1016/j.agee.2020.107216

Sun, J. N., Yang, R. Y., Zhu, J. J., Zhou, C. X., Yang, M., Pan, Y. H., et al. (2019). Contrasting Effects of Corn Straw Biochar on Soil Water Infiltration and Retention at Tilled and Compacted Bulk Densities in the Yellow River Delta. *Can. J. Soil Sci.* 99, 357–366. doi:10.1139/cjss-2019-0004

Titouna, D., and Bougoul, S. (2013). Simulation Model on Water and Solute Transport in Two Types of Rockwool. *J. Plant Nutr.* 36, 429–442. doi:10.1080/01904167.2012.748063

Wang, J. F., Wang, Z. Z., Gu, F. X., Liu, H., Kang, G. Z., Feng, W., et al. (2021). Tillage and Irrigation Increase Wheat Root Systems at Deep Soil Layer and Grain Yields in Lime Concretion Black Soil. *Scientific Rep.* 11, 6394. doi:10.1038/s41598-021-85588-6

Wang, T. T., Stewart, C. E., Ma, J. B., Zheng, J. Y., and Zhang, X. C. (2017). Applicability of Five Models to Simulate Water Infiltration into Soil with Added Biochar. *J. Arid Land* 9, 701–711. doi:10.1007/s40333-017-0025-3

Wanko, A., Laurent, J., Bois, P., Mosé, R., Wagner-Kocher, C., Bahlouli, N., et al. (2016). Assessment of Rock Wool as Support Material for On-Site Sanitation: Hydrodynamic and Mechanical Characterization. *Environ. Technol.* 37, 369–380. doi:10.1080/09593330.2015.1069901

Wasko, C., and Nathan, R. (2019). The Local Dependency of Precipitation on Historical Changes in Temperature. *Clim. Change* 156, 105–120. doi:10.1007/s10584-019-02523-5

Werdin, J., Conn, R., Fletcher, T. D., Rayner, J. P., Williams, N. S. G., and Farrell, C. (2021). Biochar Particle Size and Amendment Rate Are More Important for Water Retention and Weight of green Roof Substrates Than Differences in Feedstock Type. *Ecol. Eng.* 171, 106391. doi:10.1016/j.ecoleng.2021.106391

Winkler, K., Fuchs, R., Rounsevell, M., and Herold, M. (2021). Global Land Use Changes Are Four Times Greater Than Previously Estimated. *Nat. Commun.* 12, 2501. doi:10.1038/s41467-021-22702-2

Yang, J. H., Liu, H. Q., Lei, T. W., Rahma, A. E., Liu, C. X., and Zhang, J. P. (2021). Effect of Straw-Incorporation into Farming Soil Layer on Surface Runoff under Simulated Rainfall. *Catena* 199, 105082. doi:10.1016/j.catena.2020.105082

Yao, J. J., Cheng, J. H., Zhou, Z. D., Sun, L., and Zhang, H. J. (2018). Effects of Herbaceous Vegetation Coverage and Rainfall Intensity on Splash Characteristics in Northern China. *Catena* 167, 411–421. doi:10.1016/j.catena.2018.05.019

Yu, P. F., Li, T. X., Fu, Q., Liu, D., Hou, R. J., and Zhao, H. (2021). Effect of Biochar on Soil and Water Loss on Sloping Farmland in the Black Soil Region of Northeast China during the Spring Thawing Period. *Sustainability* 13, 1460. doi:10.3390/su13031460

Zhang, F. B., Huang, C. H., Yang, M. Y., Zhang, J. Q., and Shi, W. Y. (2019). Rainfall Simulation Experiments Indicate that Biochar Addition Enhances Erosion of Loess-Derived Soils. *Land Degrad. Develop.* 30, 2272–2286. doi:10.1002/ldr.3399

Zhang, J. L., Zhou, L. L., Ma, R. M., Jia, Y. F., Yang, F., Zhou, H. Y., et al. (2019). Influence of Soil Moisture Content and Soil and Water Conservation Measures on Time to Runoff Initiation under Different Rainfall Intensities. *Catena* 182, 104172. doi:10.1016/j.catena.2019.104172

Zhao, W., Cao, T., Dou, P., Sheng, J., and Luo, M. (2019). Effect of Various Concentrations of Superabsorbent Polymers on Soil Particle-Size Distribution and Evaporation with Sand Mulching. *Sci. Rep.* 9, 3511. doi:10.1038/s41598-019-39412-x

Zhao, X., Huang, J., Gao, X., Wu, P., and Wang, J. (2014). Runoff Features of Pasture and Crop Slopes at Different Rainfall Intensities, Antecedent Moisture Contents and Gradients on the Chinese Loess Plateau: A Solution of Rainfall Simulation Experiments. *Catena* 119, 90–96. doi:10.1016/j.catena.2014.03.007

Zhou, B. B., Chen, X. P., and Henry, L. (2020). The Effect of Nano-Biochar on Soil, Water, and Nutrient Loss of a Sloping Land with Different Vegetation Covers on Loess Plateau of China. *Appl. Ecol. Environ. Res.* 18, 2845–2861. doi:10.15666/aeer/1802_28452861

Conflict of Interest: The authors declare that the research was conducted in the absence of any commercial or financial relationships that could be construed as a potential conflict of interest.

Publisher's Note: All claims expressed in this article are solely those of the authors and do not necessarily represent those of their affiliated organizations, or those of the publisher, the editors, and the reviewers. Any product that may be evaluated in this article, or claim that may be made by its manufacturer, is not guaranteed or endorsed by the publisher.